

Introduction

Reliable wind power generation forecasting is crucial to:

- Meet energy demand through renewable power sources.
- Energy trading of future excess power.
- Design of Investment strategies.

We propose a parametric forecast error model to:

- Simulate forecast error and quantify its uncertainty.
- Calibrate a forecast model for optimal dispatch of electric power.

This model is based on:

- Parametric Stochastic Differential Equations.
- Approximate Maximum Likelihood based on continuous optimization.

The result is a skewed stochastic process that simulates the uncertainty of wind power forecasts accounting for maximum power production limit and other temporal effects. We apply the model to historical Uruguayan data and forecasts (2016-2017).

Model

Phenomenological Model

Let X_t be the wind power generation forecasts stochastic process defined by the following parameterized stochastic differential equation (SDE),

$$\begin{aligned} dX_t &= a(X_t; \theta) dt + b(X_t; \theta) dW_t \quad t > 0 \\ X_0 &= X_0 \end{aligned} \quad (1)$$

- $a(\cdot; \theta) : [0, 1] \rightarrow \mathbb{R}$ a drift function.
- $b(\cdot; \theta) : [0, 1] \rightarrow \mathbb{R}$ a diffusion function.
- θ : a vector of parameters.
- W_t : Standard Wiener random process in \mathbb{R} .

Physical Constrains

Let p_t be a numerical wind power forecast, which is an input to this approach. Then the model is given by the following Itô stochastic differential equation,

$$\begin{aligned} dX_t &= \dot{p} dt - \theta_t (X_t - p_t) dt + b(X_t; \theta) dW_t \quad t > 0 \\ X_0 &= x_0 \end{aligned} \quad (2)$$

As the installed power production capacity is limited, we normalize with respect to the installation power. Thus our process must be limited to the range $[0, 1]$. To enforce this constraint, we must have drift and diffusion control.

Diffusion Control:

The physical constraint is respected by choosing diffusion coefficient $b(x; \theta) = \sqrt{2\theta_t \alpha p_t (1 - p_t) x (1 - x)}$ that is zero on the boundaries of $[0, 1]$.

Drift Control:

X_t remains in $[0, 1]$ a.s. by choosing θ_t as follows,

$$\theta_t = \max \left(\theta_0, \frac{|\dot{p}_t|}{\min(p_t, 1 - p_t)} \right) \quad (3)$$

Change of Variables:

In order to avoid differentiation of the forecast \dot{p}_t and simplify, we apply a change of variables

$$V_t = X_t - p_t$$

Then model becomes,

$$\begin{aligned} dV_t &= -\theta_t V_t dt + \sqrt{2\theta_t \alpha p_t (1 - p_t) (V_t + p_t) (1 - V_t - p_t)} dW_t \quad t > 0 \\ V_0 &= v_0 \end{aligned} \quad (4)$$

with

$$\theta_t = \max \left(\theta_0, \frac{|\dot{p}_t|}{\min(p_t, 1 - p_t)} \right) \quad (5)$$

Where

- p_t : Numerical wind power production forecast.
- $\theta_0 > 0$: Mean reversion parameter.
- $\alpha > 0$: Variability parameter.

Inference

Likelihood

The SDE above defines the stochastic process V_t which can be characterized by its transition density.

Consider a set of M paths with N observations each, $V^{M,N} = \{V_{M,N}^1, V_{M,N}^2, \dots, V_{M,N}^M\}$ observed in intervals of Δ_N . Since V_t is Markovian, the likelihood function is given by product of its transition densities.

$$\mathcal{L}(\theta; V) = \prod_{j=1}^M \prod_{i=1}^N \rho(V_{j,i+1} | V_{j,i}, \theta) p(V_{j,0}) \quad (6)$$

Approximate Likelihood

Solving for transition densities of the process V_t requires solving the Fokker-Planck equation at every step which is computationally prohibitive. A common choice is performing a Gaussian approximation of the transition densities, but this is inappropriate here due to physical constraints.

Therefore, we propose an approximate likelihood inspired by the stationary distribution of the process X_t which is a Beta distribution for a constant forecast p_t . Additionally, as the process X_t and p_t take on values in $[0, 1]$, then V_t takes on values in $[-1, 1]$. Therefore, it is natural to use a Beta distribution with compact support on $[-1, 1]$.

Moment Matching

To approximate the transition densities of the process V_t , we match its moments with the shape parameters of the Beta distribution using Itô's formula.

The moments of the process V_t are given by,

$$\begin{aligned} \frac{dm_1(t_n)}{dt} &= -\theta_t m_1(t_n) \\ \frac{dm_2(t_n)}{dt} &= -2m_2(t_n)[\theta_t + \alpha \theta_t p_t (1 - p_t)] \\ &\quad + 2m_1(t_n)[\alpha \theta_t p_t (1 - p_t)(1 - 2p_t)] \\ &\quad + 2\alpha \theta_t p_t^2 (1 - p_t)^2 \end{aligned} \quad (7)$$

with initial conditions, $m_1(t_{n-1}) = v_{n-1}$ and $m_2(t_{n-1}) = v_{n-1}^2$.

Data

We apply the model to Uruguayan wind power generation data and their corresponding numerical wind power production forecast.

The wind power generation data set contains hourly samples of aggregated wind power production throughout the country. Each sample path contains 72 hourly observations and we have a total of 1217 sample paths spanning the year 2016 to 2017 (87,624 data points).

The numerical wind power generation forecast set contains 1217 forecasts of the wind power generation corresponding to the actual wind power generation data set mentioned above.

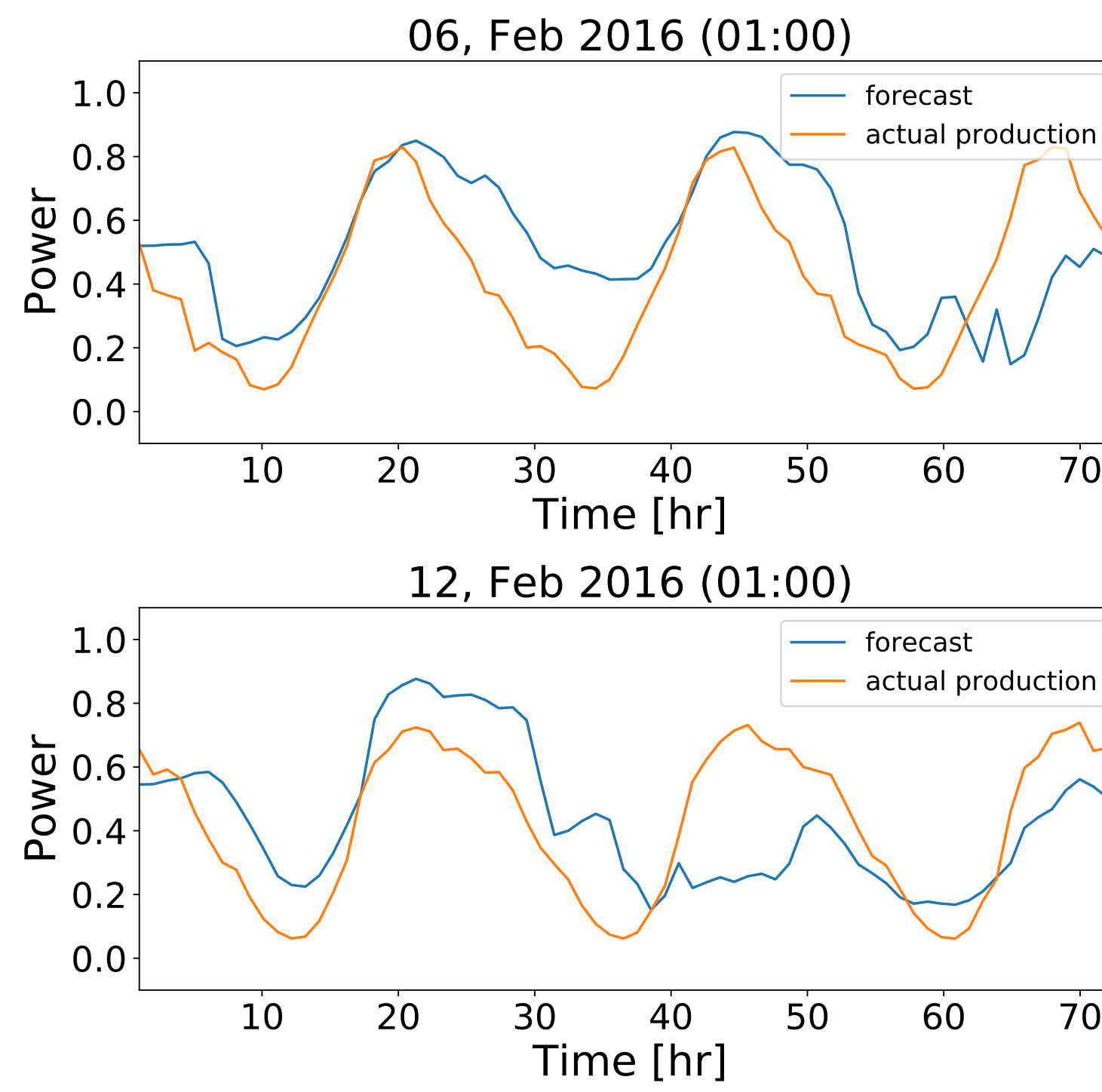


Figure 1: Examples of wind power generation from the data set along with the wind power generation forecast.

Methodology

Optimization

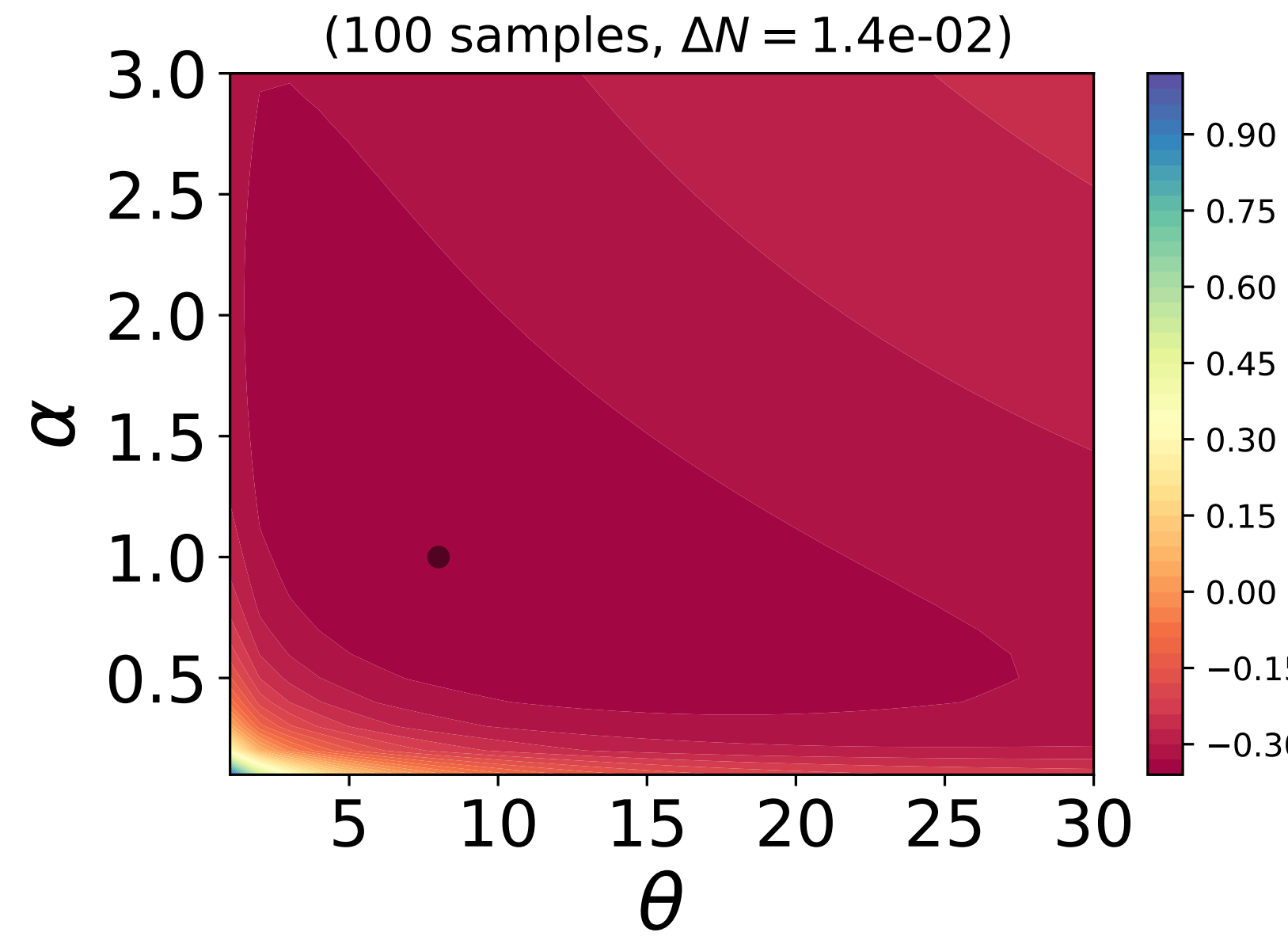


Figure 2: Contour plot of the log-likelihood with only 100 sample paths, point of optimality $(\theta_0^*, \alpha^*) \approx (8, 1)$ indicated by the black dot.

- We optimize using L-BFGS algorithm constrained to the positive quadrant.

The ellipse defined by the Hessian of the log-likelihood shrinks at a fast rate as shown in Figure (3). The contours of the log-likelihood can be seen in Figure (2).

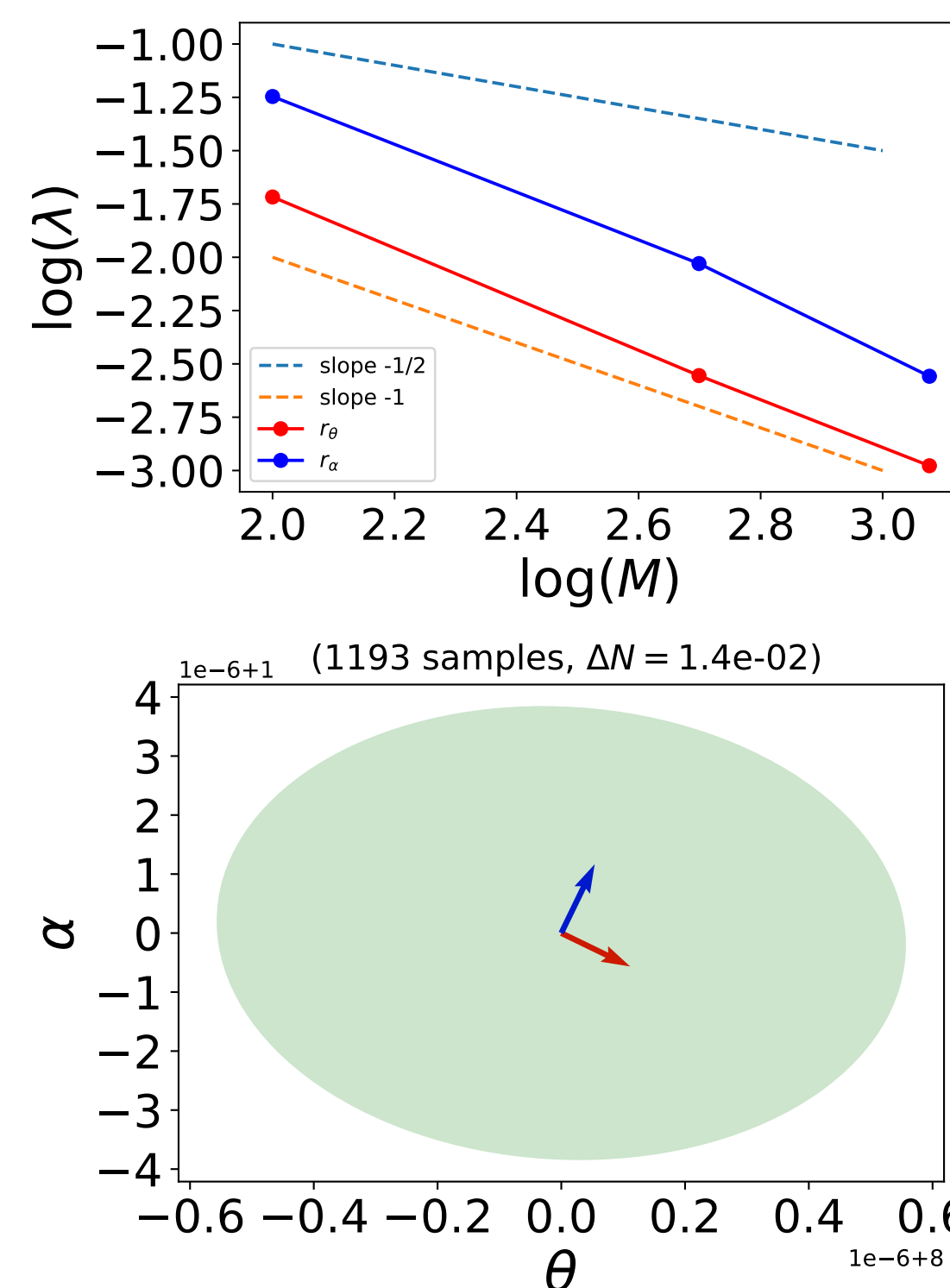


Figure 3: Left: Shrinkage of the ellipse determined by the Hessian matrix of the log-likelihood around the point of optimality $(\theta_0^*, \alpha^*) \approx (8, 1)$ (Axis are not in natural scale, arrows only to eigenvector direction). Right: Convergence of the major and semi-axis of the ellipse of the Hessian of the log-likelihood at the point optimality $(\theta_0^*, \alpha^*) \approx (8, 1)$. Note that it is slightly faster than the expected rate of $1/\sqrt{M}$. This is due to the correlation structure of the process V_t , thus a path may act as more than one uncorrelated sample.

Results

We are able to obtain the parameters based on the complete data sets mentioned earlier. The parameters are given by $(\theta^*, \alpha^*) \approx (8, 1)$.

In Figure (4) and (6), we simulate sample forecast errors using the optimal parameters $(\theta_0^*, \alpha^*) \approx (8, 1)$ and obtain the associated confidence bands empirically using 1000 sample paths for each forecast.

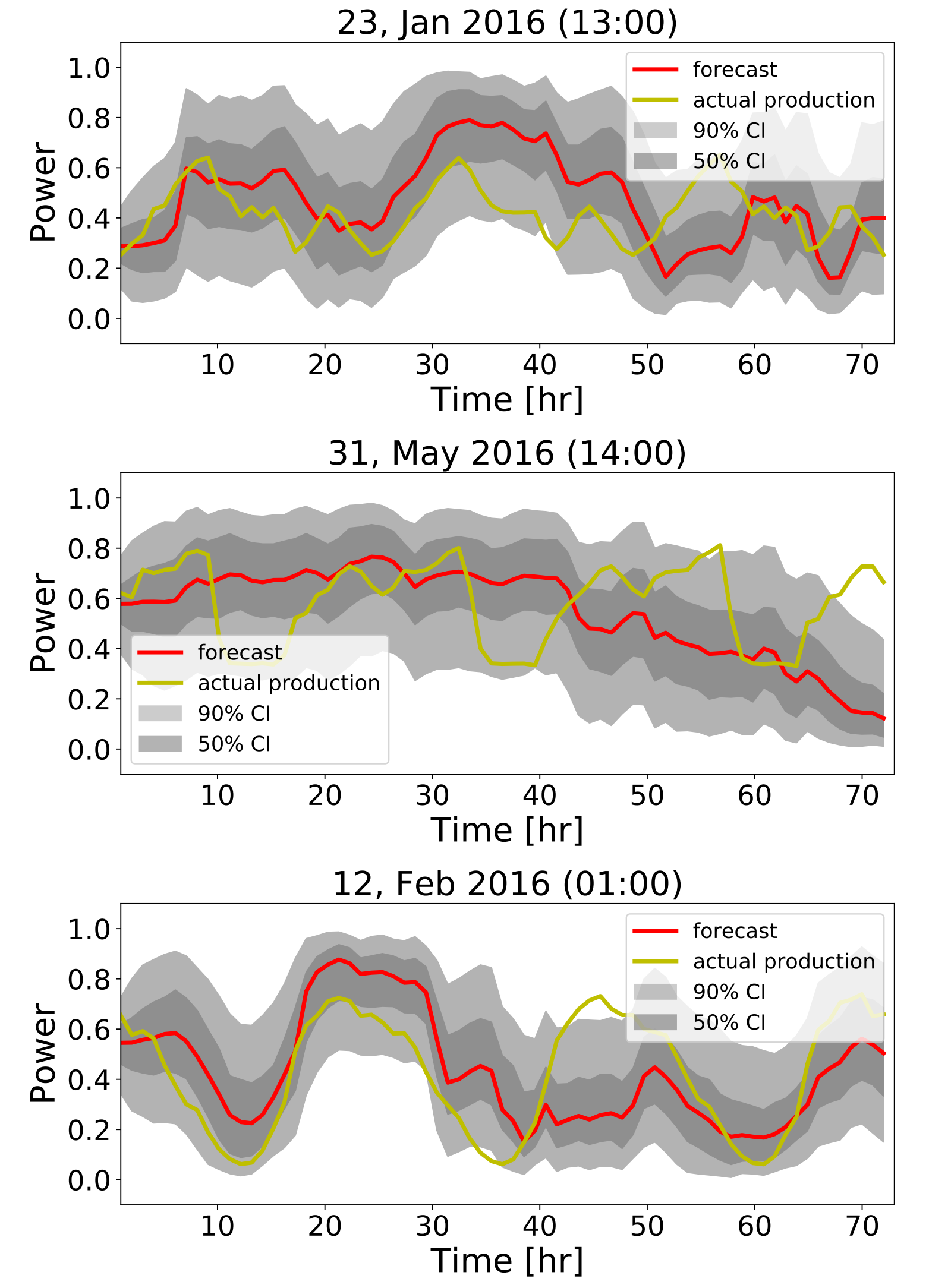


Figure 4: Examples of confidence bands obtained for the full 72 hour forecasts. We can see that the model captures the fluctuations in the actual production with non-trivial and asymmetric confidence intervals.

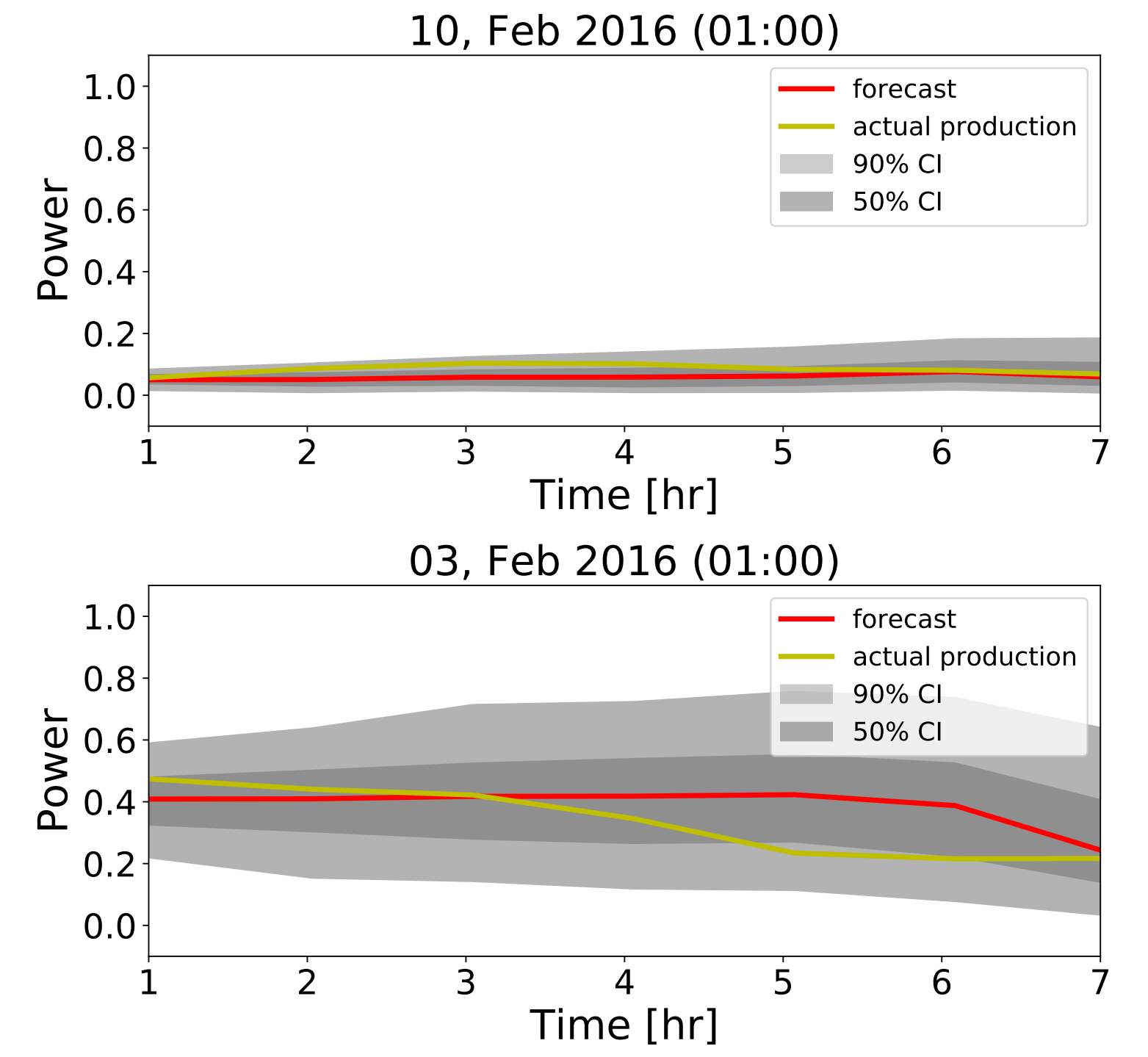


Figure 5: Examples of confidence bands obtained for the first 6 hours of the forecasts. This is important as this specific forecasting company computes a new forecast every 6 hours for reliability.

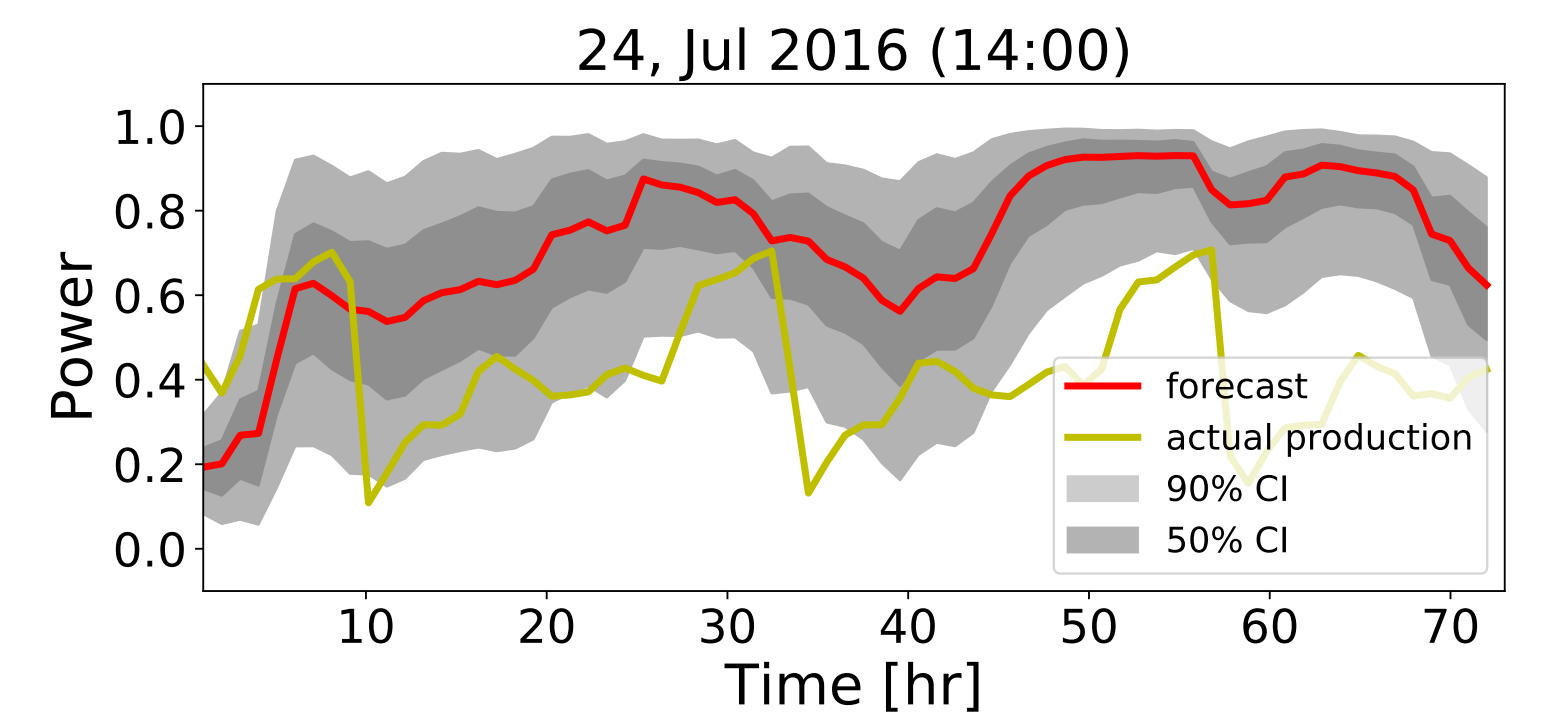


Figure 6: Examples of omitted data which corresponds to production control and manual energy management decisions. In this example, wind power production was repeatedly curtailed at around 2 AM which is a period of low power demand. Automatic detection of such scenarios is to be incorporated in future works.

Conclusions

In this project, we have proposed a model based on SDE's to quantify uncertainties in wind power generation forecasts. It has the following advantages:

- Represents and quantifies uncertainty in wind power forecasts.
- It is forecast technology agnostic.
- Takes into account physical constrains and the skew-symmetric nature of forecast error.
- Provides a basis for decision making in the optimal dispatch of electric power.

References

- [1] Elkantassi, S., Kalligiannaki, E., & Tempone, R. (2017). Inference And Sensitivity In Stochastic Wind Power Forecast Models. Proceedings of the 2nd International Conference on Uncertainty Quantification in Computational Sciences and Engineering (UNCCECOMP 2017). doi:10.7712/120217.5377.16899